SWIRLING FLOW OVER AN OSCILLATORY STRETCHABLE DISK

S. Munawar *

Department of Informatics and Systems
School of Science & Technology
University of Management & Technology
Lahore 54000, Pakistan

A. Ali

Department of Mathematics and Natural Sciences
Prince Mohammad Bin Fahd University
Al Khobar 31952, Saudi Arabia

Department of Mathematics
Quaid-i-Azam University
Islamabad 44000, Pakistan

N. Saleem

Department of Mathematics and Natural Sciences
Prince Mohammad Bin Fahd University
Al Khobar 31952, Saudi Arabia

A. Naqeeb

Department of Mathematics
Karakoram International Univeristy
Gilgit-Baltistan, Pakistan

ABSTRACT

In this work a numerical investigation has been conducted to study the unsteady oscillatory flow of a viscous fluid induced by a swirling disk. The disk stretches radially with the time-based sinusoidal oscillations. The governing equations for the three-dimensional boundary layer-flow are normalized using a suitable set of similarity transformations. The normalized partial differential equations are then solved numerically using a finite difference scheme by altering the semi-infinite domain to a finite domain. The effects of various imperative parameters on the oscillatory flow are discussed with graphs and tables.

Keywords: Oscillatory flow, Viscous fluid, Rotating disk, Numerical solution.

1. INTRODUCTION

The behavior of boundary-layer flows over the rotating and stretching surfaces is one of the interesting topics to be studied as it has great practical importance in engineering and industrial processes. Such type of flow phenomena occur in fuel and aerodynamic industries, biomechanics, extrusion and condensation processes, thermal-power generating systems, gas turbines, medical equipment, *etc.* Accordingly, the theoretical learning of such flow phenomena has been achieved a great attention from scientists and engineers for last few years. The work on such type of flows was initiated by Sakiadis [1] who investigated the viscous flow over moving surfaces. The flow of a viscous fluid caused by a stretching surface was examined by Crane [2]. Afterwards, Wang [3] extended the work by considering three-dimensional flow caused by a stretching sheet using a numerical technique. Later on, numerous authors [4-10] inspired by the work of Crane [2] explored the flow over stretching surfaces under several interesting physical features such as porous medium, suction and injection at stretching sheet, electrically conducting fluid, unsteadiness and viscoelastic nature of fluid. The flow caused by the periodical oscillation is always important for it has numerous practical applications in variety of bio-engineering problems and in the aerodynamics of fluttering airfoil and helicopter rotor. In this regard, the flow over oscillatory stretching sheet was initially considered by Wang [11] who calculated the perturbation solution by taking large frequency of oscillations. Rajagopal *et al*. [12] studied the oscillatory motion of electrically conducting Walters' liquid B' model fluid over an impermeable stretching sheet in porous medium and obtained the perturbation solution by taking small amplitude of oscillations. Motivated by the work of Wang [11], Abbas *et al*. [13] investigated the slip effects of a viscous fluid over an oscillatory stretching flat plate. Munawar *et al*. [14] numerically studied the oscillatory flow of a viscous fluid over an oscillatory stretching cylinder.

Von Kármán [15] is the first one who initiated the theoretical study on the rotating disk flow problem and showed that the Navier-Stokes equations for the three-dimensional flow can be reduced to ordinary differential equations using the self-similar transformations. Later on, the Kármán's problem was vastly explored by various authors [16-20] by assuming various physical assumptions. Cochran [16] obtained more accurate solution of the problem by numerical integration of

* Corresponding author (sufian.munawar@hotmail.com)

DOI : 10.1017/jmech.2014.37
Copyright © 2014 The Society of Theoretical and Applied Mechanics, R.O.C.
https://doi.org/10.1017/jmech.2014.37 Published online by Cambridge University Press

governing equations. The effect of uniform suction and injection at the surface of disk was taken into account by Stuart [17] and obtained the numerical results for small values of suction parameter and series solution for large values. A numerical scheme was used by Sparrow and Gregg [18] to acquire the solution for both suction and blowing cases. Kuiken [19] utilized the method of asymptotic expansion to obtain the solution of the problem for large values of blowing. Same problem was considered by Ackroyd [20] who calculated a series solution which was legitimated for large values of suction and small values of injection. Moreover, magnetic effects on the flow for the particular problem were scrutinized by various authors [21-24]. Axisymmetric flow of a viscoelastic fluid over a radially stretching disk was considered by Ariel [25] who obtained the perturbation solution for small Deborah number and asymptotic solution for large Deborah number. The work of Ariel was extended by Sajid *et al*. [26] who obtained an analytic solution for unsteady flow and heat transfer over a radially stretching sheet. Fang and Zhang [27] extended the problem of Ariel [25] by taking a viscous fluid between two infinite stretching disks fixed at a finite distance. Munawar *et al*. [28] discussed the slip effects on the flow between two stretchable disks with the help of optimal HAM. Three-dimensional flow over a stretching and rotating disk was investigated by Fang [29], who discussed the cases of a stretchable disk and a rotating stretchable disk and also the case when rotating rate is much larger than the stretching rate. Recently, Munawar *et al*. [30] obtained two solution branches numerically for the stagnation point flow over rotating a rotating disk impinges the forthcoming fluid.

Motivated by the above mentioned studies the purpose of current study is to investigate the unsteady oscillatory boundary-layer flow over a rotating and oscillating stretchable disk. The time dependent sinusoidal oscillations are taken into account in radial direction. The numerical solution is obtained for the three-dimensional flow problem using a finite difference method.

2. MATHEMATICAL FORMULATION

Consider an unsteady axisymmetric flow of a viscous incompressible fluid caused by the impulsive motion of a rotating stretchable disk. The disk is immersed in the fluid at $z = 0$ and rotating about its axis $r = 0$ with a constant angular velocity γ. Moreover, the disk stretches in radial direction periodically with the sinusoidal oscillations of constant amplitude ε. For an axisymmetric flow the change with respect to the polar angle θ vanishes. The governing equations for the considered flow take the form

$$\frac{\partial u}{\partial r}+\frac{u}{r}+\frac{\partial w}{\partial z}=0\,, \tag{1}$$

$$\frac{\partial u}{\partial t}+u\frac{\partial u}{\partial r}-\frac{v^2}{r}+w\frac{\partial u}{\partial z}=-\frac{1}{\rho}\frac{\partial p}{\partial r}+\nu\left[\frac{\partial^2 u}{\partial r^2}+\frac{\partial}{\partial r}\left(\frac{u}{r}\right)+\frac{\partial^2 u}{\partial z^2}\right], \tag{2}$$

$$\frac{\partial v}{\partial t}+u\frac{\partial v}{\partial r}+\frac{uv}{r}+w\frac{\partial v}{\partial z}=\nu\left[\frac{\partial^2 v}{\partial r^2}+\frac{\partial}{\partial r}\left(\frac{v}{r}\right)+\frac{\partial^2 v}{\partial z^2}\right], \tag{3}$$

$$\frac{\partial w}{\partial t}+u\frac{\partial w}{\partial r}+w\frac{\partial w}{\partial z}=-\frac{1}{\rho}\frac{\partial p}{\partial z}+\nu\left[\frac{\partial^2 w}{\partial r^2}+\frac{1}{r}\frac{\partial w}{\partial r}+\frac{\partial^2 w}{\partial z^2}\right], \tag{4}$$

subject to the boundary conditions (for $t > 0$)

$$\begin{aligned} &u(r,z;t)=ar(1+\varepsilon\cos\omega t)\,,\ v(r,z;t)=\gamma r\,,\\ &w(r,z;t)=0\,,\ \text{at}\ \ z=0\,, \end{aligned} \tag{5}$$

$$\begin{aligned} &u(r,z;t)=0\,,\ v(r,z;t)=0\,,\\ &w(r,z;t)=0\,,\ \text{at}\ \ z\to\infty\,, \end{aligned} \tag{6}$$

and the initial conditions

$$u=v=w=0\,,\ \text{at}\ \ t=0\ \ \text{for all}\ r\ \text{and}\ z\,. \tag{7}$$

To normalize the above system of Eqs. (1) ~ (7) the following Von Kármán type of similarity transformations are used:

$$\left.\begin{aligned} &u=arF'(z^*,t^*)\,,\ v=arG(z^*,t^*)\,,\ w=-2\sqrt{a\nu}F(z^*,t^*)\,,\\ &z^*=\sqrt{\frac{a}{\nu}}z\,,\ t^*=\omega t\,,\ p=\rho a\nu P(z^*,t^*)\,. \end{aligned}\right\} \tag{8}$$

Using the above transformations in Eqs. (1) ~ (6) and dropping the asterisks, Eq. (1) satisfies identically and we left with the following system of partial differential equations:

$$F'''+2FF''-(F')^2+G^2-StF_t'=0\,, \tag{9}$$

$$G''+2FG'-2F'G-StG_t=0\,, \tag{10}$$

with the boundary conditions

$$\begin{aligned} &F(0,t)=0,\ F'(0,t)=1+\varepsilon\cos t\,,\\ &G(0,t)=\frac{\gamma}{a}=\Omega\,,\ \ P(0,t)=0\,, \end{aligned} \tag{11}$$

$$F'(\infty,t)=0,\ G(\infty,t)=0\,, \tag{12}$$

where prime denotes the differentiation with respect to dimensionless variable z, the subscript t denotes the differentiation with respect to dimensionless time t, $St = \omega/a$ the Strouhal number, γ the angular velocity of disk and Ω the swirl parameter with $\Omega > 1$ implies that the rate of angular velocity is greater than the stretching rate, for $\Omega < 1$ the stretching rate is greater than rotating velocity and $\Omega = 0$ corresponds to no rotation. The pressure distribution turns out to be

$$P=2St\int_0^\infty F_t\,dz-2F^2-2F'\,. \tag{13}$$

The shear stresses τ_{zr} and $\tau_{z\theta}$ at the surface are given by

$$\begin{aligned} &\tau_{zr}=\mu\left.\frac{\partial u}{\partial z}\right|_{z=0}=\mu aRe^{1/2}F''(0,t)\,,\\ &\tau_{z\theta}=\mu\left.\frac{\partial v}{\partial z}\right|_{z=0}=\mu aRe^{1/2}G'(0,t)\,, \end{aligned} \tag{14}$$

where $\mathrm{Re}^{1/2} = ar^2/\nu$ is the local Reynolds number.

https://doi.org/10.1017/jmech.2014.37 Published online by Cambridge University Press

3. NUMERICAL SOLUTION

To acquire the numerical solution of Eqs. (9) ~ (12), we used the finite difference method (FDM). For this we first convert the semi-infinite domain $z \in [0,\infty)$ into a finite domain $\zeta \in [0,1]$ by using the following transformation:

$$\zeta = 1/1+z\,. \tag{15}$$

Using (15), Eqs. (9) ~ (12) transform into the following set of partial differential equations in a bounded domain:

$$\zeta^6 \frac{\partial^3 F}{\partial \zeta^3} + (6\zeta^5 - 2\zeta^4 F)\frac{\partial^2 F}{\partial \zeta^2} + \left(6\zeta^4 - 4\zeta^3 F + \zeta^4 \frac{\partial F}{\partial \zeta}\right)\frac{\partial F}{\partial \zeta} - G^2 - St\zeta^2 \frac{\partial^2 F}{\partial t \partial \zeta} = 0\,, \tag{16}$$

$$\zeta^4 \frac{\partial^2 G}{\partial \zeta^2} + 2\zeta^2(\zeta - F)\frac{\partial G}{\partial \zeta} + 2\zeta^2 \frac{\partial F}{\partial \zeta} G - St\frac{\partial G}{\partial t} = 0\,, \tag{17}$$

$$\left.\frac{\partial F}{\partial \zeta}\right|_{\zeta=0} = 0,\ G(0,t) = 0\,,\ F(1,t) = 0\,,$$
$$\left.\frac{\partial F}{\partial \zeta}\right|_{\zeta=1} = -1 - \cos t\,,\ G(1,t) = \Omega\,. \tag{18}$$

Now Eqs. (16) and (17) along with the boundary data (18) are solved with the help of finite difference scheme. In order to linearize Eqs. (16) and (17), we replace the linear terms at $(k + 1)$th time step and the nonlinear terms at kth time step and use forward difference approximation for the time derivative $\partial / \partial t$ so that the linearized system takes the form

$$\zeta^6 \frac{\partial^3 F^{(k+1)}}{\partial \zeta^3} + 6\zeta^5 \frac{\partial^2 F^{(k+1)}}{\partial \zeta^2} + 6\zeta^4 \frac{\partial F^{(k+1)}}{\partial \zeta} - \frac{St}{\Delta t}\zeta^2\left(\frac{\partial F^{(k+1)}}{\partial \zeta} - \frac{\partial F^{(k)}}{\partial \zeta}\right) = -\zeta^4\left(\frac{\partial F^{(k)}}{\partial \zeta}\right)^2 + 2\zeta^4 F^{(k)}\frac{\partial^2 F^{(k)}}{\partial \zeta^2} + 4\zeta^3 F^{(k)}\frac{\partial F^{(k)}}{\partial \zeta} + \left(G^{(k)}\right)^2\,, \tag{19}$$

$$\zeta^4 \frac{\partial^2 G^{(k+1)}}{\partial \zeta^2} + 2\zeta^3 \frac{\partial G^{(k+1)}}{\partial \zeta} - \frac{St}{\Delta t} G^{(k+1)} = 2\zeta^2 F^{(k)}\frac{\partial G^{(k)}}{\partial \zeta} - 2\zeta^2 \frac{\partial F^{(k)}}{\partial \zeta} G^{(k)} - \frac{St}{\Delta t} G^{(k)}\,. \tag{20}$$

The initial values can be obtained from the initial condition at $k = 0$ as under:

$$F(\zeta, t=0) = F_j^0 = G(\zeta, t=0) = G_j^0 = 0\,. \tag{21}$$

Next we discretize the linear system of differential Eqs. (19) and (20) with respect to the spatial variable ζ into M uniformly distributed grid points as $\zeta_0 = 0$, ζ_1, ζ_2, …, ζ_M, $\zeta_{M+1} = 1$ with a grid size of $\Delta\zeta = 1/(M+1)$. To discretize spatial derivatives in Eqs. (19) and (20) we use the following second order central difference approximations for the first two derivatives:

$$\frac{\partial F}{\partial \zeta} \approx \frac{F_{j+1} - F_{j-1}}{2\Delta\zeta} + O(\Delta\zeta^2)\,, \tag{22}$$

$$\frac{\partial^2 F}{\partial \zeta^2} \approx \frac{F_{j+1} - 2F_j + F_{j-1}}{(\Delta\zeta)^2} + O(\Delta\zeta^2)\,, \tag{23}$$

and due to the two boundary conditions at $\zeta = 1$ and one at $\zeta = 0$ we use the following first order difference scheme for the third order derivative:

$$\frac{\partial^3 F}{\partial \zeta^3} \approx \frac{F_{j+2} - 3F_{j+1} + 3F_j - F_{j-1}}{(\Delta\zeta)^3} + O(\Delta\zeta)\,, \tag{24}$$

where F_j are the corresponding values of F at $\zeta_j = (j - 1)\,\Delta\zeta$ for $j = 1, 2, \ldots, M+1$. The above finite difference scheme results in a linear system of algebraic equations given by

$$A_{1j} F_{j+2}^{(k+1)} + B_{1j} F_{j+1}^{(k+1)} + C_{1j} F_j^{(k+1)} + D_{1j} F_{j-1}^{(k+1)} = E_{1j}\,, \quad \text{for } j = 2, 3, \ldots, M-2\,, \tag{25}$$

$$A_{2j} G_{j+1}^{(k+1)} + B_{2j} G_j^{(k+1)} + C_{2j} G_{j-1}^{(k+1)} = E_{2j} \quad \text{for } j = 2, 3, \ldots, M-1\,, \tag{26}$$

where

$$\left.\begin{aligned} A_{1j} &= \frac{\zeta_j^6}{(\Delta\zeta)^3}\,,\ B_{1j} = -\frac{3\zeta_j^6}{(\Delta\zeta)^3} + \frac{6\zeta_j^5}{(\Delta\zeta)^2} + \frac{3\zeta_j^4}{\Delta\zeta} - \frac{St\zeta_j^2}{2\Delta t\Delta\zeta}\,,\\ C_{1j} &= \frac{3\zeta_j^6}{(\Delta\zeta)^3} - \frac{12\zeta_j^5}{(\Delta\zeta)^2}\,,\ D_{1j} = -\frac{\zeta_j^6}{(\Delta\zeta)^3} + \frac{6\zeta_j^5}{(\Delta\zeta)^2} - \frac{3\zeta_j^4}{\Delta\zeta} + \frac{St\zeta_j^2}{2\Delta t\Delta\zeta}\,,\\ E_{1j} &= -\frac{St\zeta_j^2}{2\Delta t\Delta\zeta} F_{j+1}^{(k)} - \zeta^4\left(\frac{F_{j+1}^{(k)} - F_{j-1}^{(k)}}{2\Delta\zeta}\right)^2 + 4\zeta^3 F_j^{(k)}\left(\frac{F_{j+1}^{(k)} - F_{j-1}^{(k)}}{2\Delta\zeta}\right)\\ &\quad + 2\zeta^4 F_j^{(k)}\left(\frac{F_{j+1}^{(k)} - 2F_j^{(k)} + F_{j-1}^{(k)}}{\partial\zeta^2}\right) + \left(G_j^{(k)}\right)^2\,, \end{aligned}\right\} \tag{27}$$

$$\left.\begin{aligned} A_{2j} &= \frac{\zeta_j^4}{(\Delta\zeta)^2} + \frac{\zeta_j^3}{\Delta\zeta},\ B_{2j} = \frac{-2\zeta_j^4}{(\Delta\zeta)^2} - \frac{St}{\Delta t},\ C_{2j} = \frac{\zeta_j^4}{(\Delta\zeta)^2} - \frac{\zeta_j^3}{\Delta\zeta}\,,\\ E_{2j} &= \frac{\zeta_j^2}{\Delta\zeta} F_j^{(k)} G_{j+1}^{(k)} - \zeta_j^2\left(\frac{F_{j+1}^{(k)} - F_{j-1}^{(k)}}{\Delta\zeta}\right) G_j^{(k)} - \frac{\zeta_j^2}{\Delta\zeta} F_j^{(k)} G_{j-1}^{(k)} - \frac{St}{\Delta t} G_j^{(k)}, \end{aligned}\right\} \tag{28}$$

The above linear algebraic equations are solved using the Gaussian elimination method for different time levels $t^{(k)}$ $(= k\Delta t)$ for $k = 0, 1, 2, \ldots$ with time step Δt.

4. NUMERICAL RESULTS AND DISCUSSION

In this section, the numerical results of the problem are described by graphs and tables and the effects of

https://doi.org/10.1017/jmech.2014.37 Published online by Cambridge University Press

various parameters on velocity and shear forces are discussed physically. Figures 1 to 8 show the effect of swirl parameter Ω on the velocity profiles and frictional forces in all directions. It is observed from Fig. 1 that the dimensionless radial velocity increases as Ω increases and for Ω > 1 the radial velocity of fluid considerably exceeds from the velocity of disk. This is mainly due to the fact that as the disk rotates rapidly the centrifugal force pushes the fluid particles in radial direction. Figure 2 is plotted to see the effect of Ω on the radial velocity by keeping $z = 0.25$ for the first four periods of oscillations in the time range $0 \le t \le 4 \times 2\pi$. It is observed from here that for small time the amplitude of vibrations is small and as time precedes the amplitude increases and becomes constant as the steady state is achieved. It is also scrutinized from the figure that for small Ω the amplitude of oscillations in the radial velocity is slightly high as compared to the large Ω because more rapid rotation causes great thrust to the fluid particles in radial direction and therefore the effect of oscillations in radial direction becomes weak. Figure 3 illustrates that as Ω increases the radial shear stress also increases. Table 1 shows that the radial stress changes the sign from negative to positive which indicates that the radial velocity of fluid becomes larger as compared to the disk velocity when Ω exceeds from 5. It is further noted that for all time the radial stress demonstrates increasing behavior as swirl parameter Ω increases. Figure 4 illustrates the influence of Ω on the axial velocity and it is seen from here that as Ω increases the axial velocity also increases. The main physical reason behind this conduct of velocity is the escaping of fluid particles in radial direction due to the centrifugal force which is balanced by the particles approaching toward the disk in the negative axial direction. From Fig. 5 it is noted that as swirl parameter Ω increases the amplitude of oscillations in the axial velocity decreases. Figure 6 shows that the tangential velocity increases near the disk surface as Ω increases. From the Fig. 7 it is noticed that as Ω increases the amplitude of oscillations also augments and this is due the fact that the oscillation in radial direction also penetrates in the torsional velocity and as the swirl increases the infiltration of these oscillations also enhances by momentum transport in tangential direction. However, it is seen that the amplitude of oscillation in tangential velocity is very small as compared to the radial velocity (see for instance Fig. 2). Consequently, the frictional torque, as well as, the amplitude of oscillation in it decreases (see Fig. 8). Table 2 reports the numerical values of frictional torque for different values of Ω which shows that as Ω in increases that frictional torque decreases. This is due to the Carioles forces becoming stronger as rotation rate increases.

Figures 9 to 16 illustrate the effects of Strouhal number *St* on the flow phenomenon. Figure 9 indicates that as *St* number increases the radial velocity decreases. Figure 10 is plotted to see the effects of *St* on radial velocity against *t* at fixed $z = 0.25$. From here we observe that the effect of unsteadiness dominates and the steady state time is increasing with increasing of *St*.

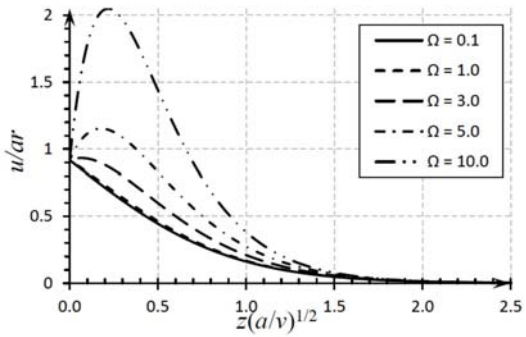


Fig. 1 Effect of swirl parameter Ω on the radial velocity *u* against *z*, when $St = 5$, $\varepsilon = 0.2$ and $t = 2$

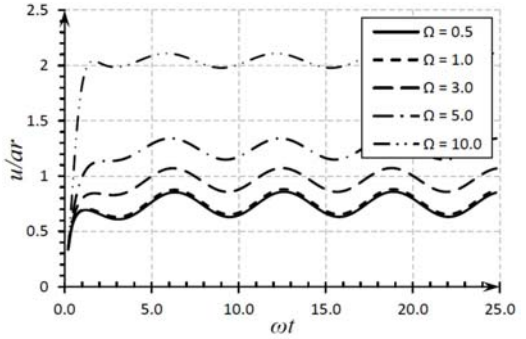


Fig. 2 Effect of swirl parameter Ω on the radial velocity *u* against *t*, when $St = 5$, $\varepsilon = 0.2$ and $z = 0.25$

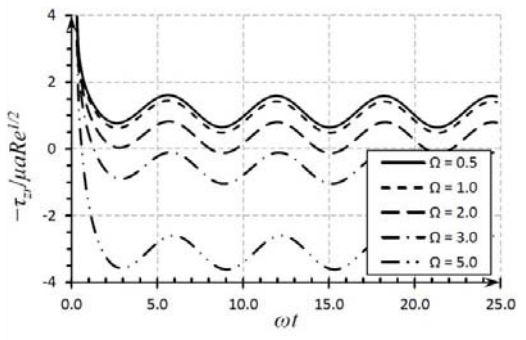


Fig. 3 Effect of swirl parameter Ω on the radial shear force τ_{zr}, when $St = 5$ and $\varepsilon = 0.2$

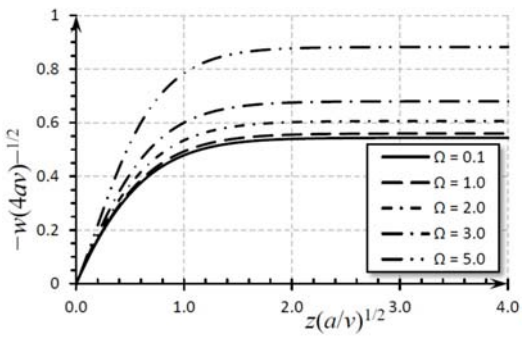


Fig. 4 Effect of swirl parameter Ω on the axial velocity *w* against *z*, when $St = 5$, $\varepsilon = 0.2$ and $t = 2$

https://doi.org/10.1017/jmech.2014.37 Published online by Cambridge University Press

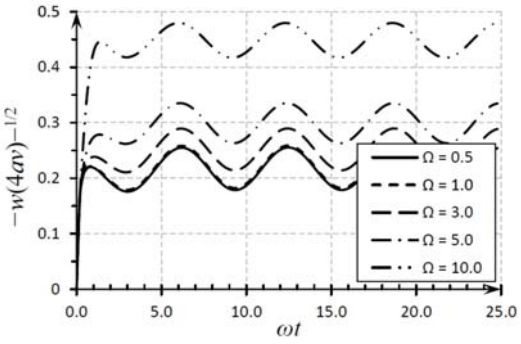


Fig. 5 Effect of swirl parameter Ω on the axial velocity w against t, when $St = 5$, $\varepsilon = 0.2$ and $z = 0.25$

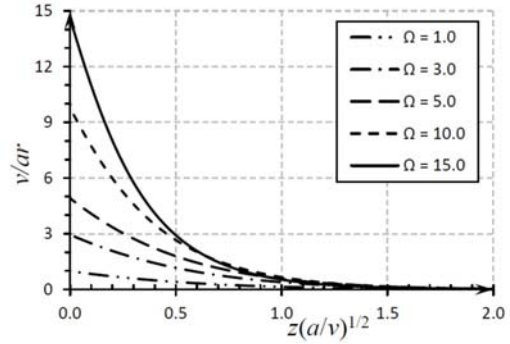


Fig. 6 Effect of swirl parameter Ω on the tangential velocity v against z, when $St = 5$, $\varepsilon = 0.2$ and $t = 2$

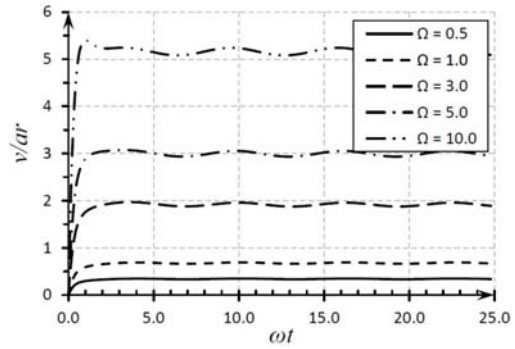


Fig. 7 Effect of swirl parameter Ω on the tangential velocity v against t, when $St = 5$, $\varepsilon = 0.2$ and $z = 0.25$

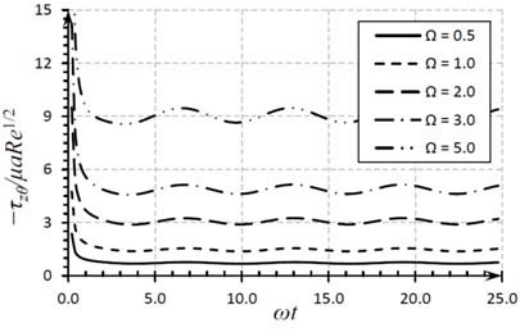


Fig. 8 Effect of swirl parameter Ω on the frictional torque $\tau_{z\theta}$ versus t, when $St = 5$ and $\varepsilon = 0.2$

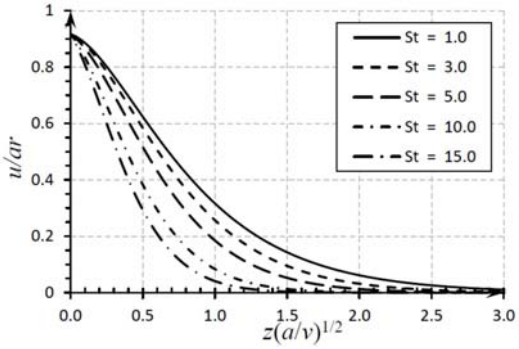


Fig. 9 Effect of St on the radial velocity u against z, when $\Omega = 2$, $\varepsilon = 0.2$ and $t = 2$

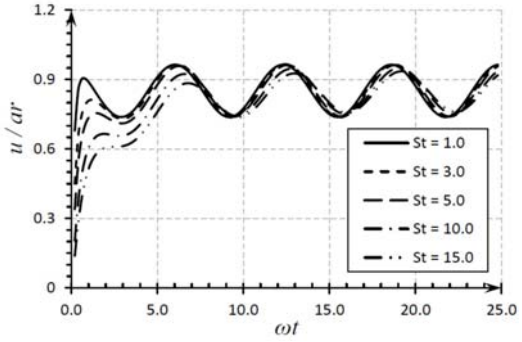


Fig. 10 Effect of St on the radial velocity u against t, when $\Omega = 2$, $\varepsilon = 0.2$ and $z = 0.25$

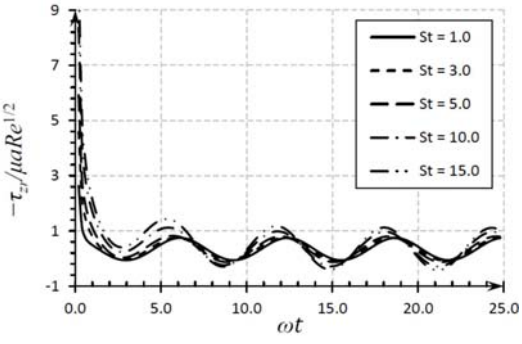


Fig. 11 Effect of St on the radial shear force τ_{zr} versus t, when $\Omega = 5$ and $\varepsilon = 0.2$

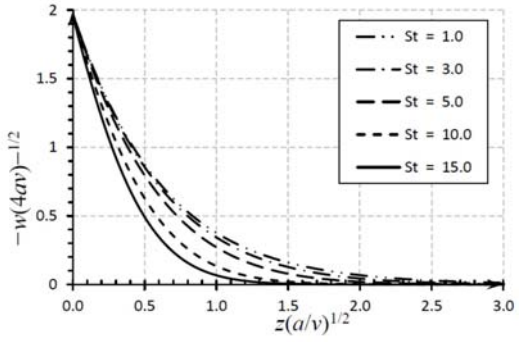


Fig. 12 Effect of St on the tangential velocity v against z, when $\Omega = 2$, $\varepsilon = 0.2$ and $t = 2$

https://doi.org/10.1017/jmech.2014.37 Published online by Cambridge University Press

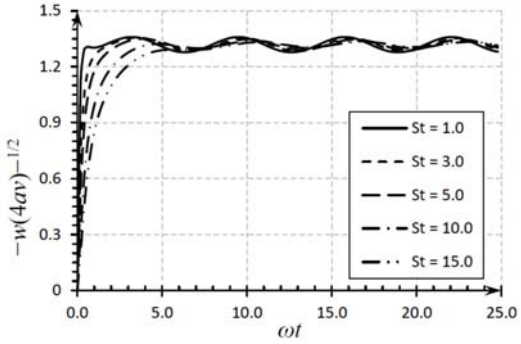


Fig. 13 Effect of *St* on the tangential velocity *v* against *t*, when Ω = 2, ε = 0.2 and *z* = 0.25

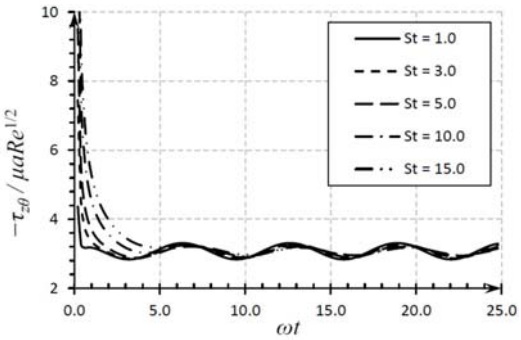


Fig. 14 Effect of *St* on the frictional torque $\tau_{z\theta}$ versus *t*, when Ω = 2 and ε = 0.2

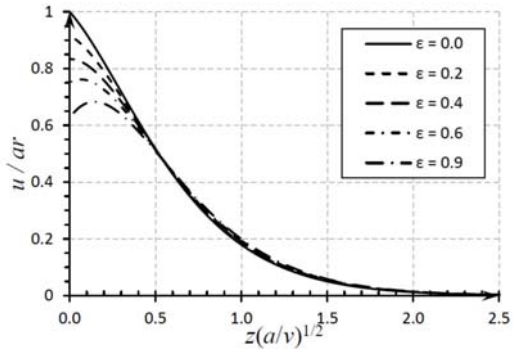


Fig. 15 Effect of ε on the radial velocity *u* against *z*, when Ω = 2, *St* = 5 and *t* = 2

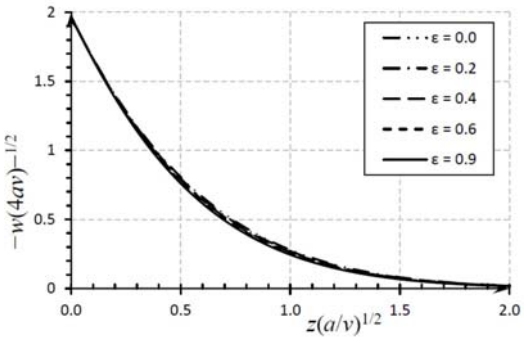


Fig. 16 Effect of ε on the tangential velocity *v* against *z*, when Ω = 2, *St* = 5 and *t* = 2

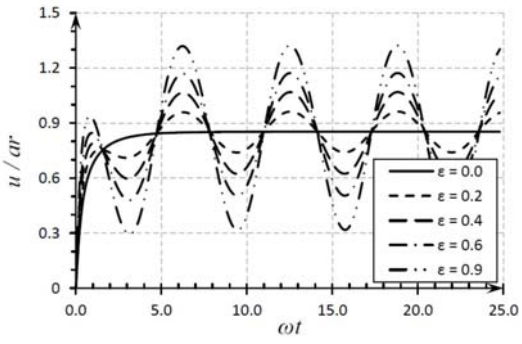


Fig. 17 Effect of ε on the radial velocity *u* against *t*, when Ω = 2, *St* = 5 and *z* = 0.25

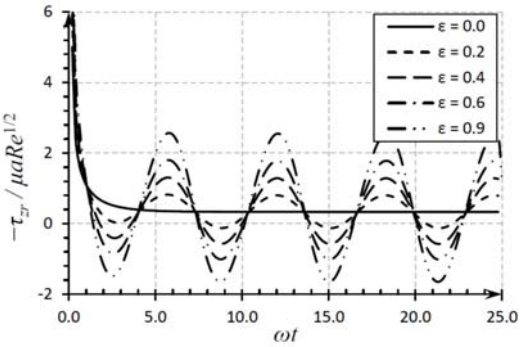


Fig. 18 Effect of ε on the radial shear force τ_{zr} versus *t*, when Ω = 5 and *St* = 5

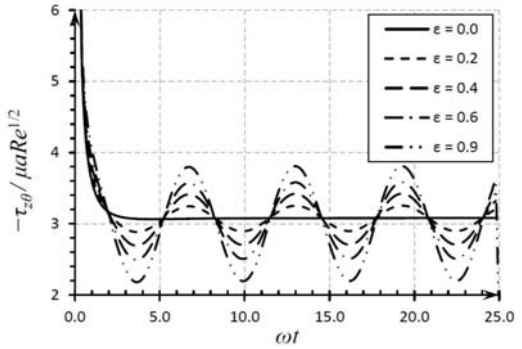


Fig. 19 Effect of ε on the frictional torque $\tau_{z\theta}$ versus *t*, when Ω = 2 and *St* = 5

Effect of *St* on the radial shear force is demonstrated in Fig. 11, from here it is noted that the amplitude of radial shear force increases as *St* increases. Table 1 shows the numerical values of the radial stress for different values of *St* which demonstrates decreasing trend in the stress as *St* increases. The effect of *St* on rotating velocity can be scrutinized from Fig. 12 and it is noticed from the figure that the transversal velocity decreases and it is due to the strong inertial forces which cause great resistance in momentum transport. Figure 13 illustrates the effects of *St* on rotating velocity versus *t* and it is observed from the figure that the amplitude of oscillations decreases by increasing *St* and the steady state time is achieved after some delay. The frictional torque *G*'(0, *t*) increases with *St* for small time and when steady state time is achieved the amplitude of oscillation in frictional torque decreases by increasing

https://doi.org/10.1017/jmech.2014.37 Published online by Cambridge University Press

Table 1 Numerical values of dimensionless radial shear stress τ_{zr} for different values of physical parameters at different time levels

Ω	*St*	ε	$t = 0.5$	$t = 2$	$t = 4$	$t = 6$
0.1	5	0.2	–2.8024	–0.9809	–1.1194	–1.6621
1			–2.7201	–0.8029	–0.9014	–1.4441
3			–2.0554	0.5856	0.6943	–0.0882
5			–0.7275	3.1349	3.3525	2.5887
10			5.4720	12.7023	12.7888	11.6770
2	1		–0.9969	–0.1527	–0.0815	–0.7361
	3		–1.8632	–0.1738	–0.1662	–0.7625
	5		–2.4708	–0.2721	–0.2717	–0.8297
	10		–3.5773	–0.5197	–0.5474	–1.0766
	15		–4.4209	–0.7244	–0.7921	–1.3417
	5	0	–2.0596	–0.6358	–0.4027	–0.3529
		0.1	–2.2636	–0.4535	–0.3348	–0.5894
		0.3	–2.6811	–0.0914	–0.2136	–1.0739
		0.5	–3.1112	0.2677	–0.1121	–1.5739
		0.7	–3.5537	0.6240	–0.0314	–2.0889

Table 2 Numerical values of dimensionless frictional torque $\tau_{z\theta}$ for different values of physical parameters at different time levels

Ω	*St*	ε	$t = 0.5$	$t = 2$	$t = 4$	$t = 6$
0.1	5	0.2	–0.2507	–0.1560	–0.1366	–0.1492
1			–2.5075	–1.5706	–1.3881	–1.5195
3			–7.5366	–4.9411	–4.6000	–5.0475
5			–12.6078	–8.8998	–8.6470	–9.3577
10			–25.6533	–21.9053	–21.7214	–22.8028
2	1		–3.3253	–3.0232	–2.8905	–3.2805
	3		–4.2070	–3.0776	–2.8779	–3.2268
	5		–5.0186	–3.2003	–2.8963	–3.1816
	10		–6.6573	–3.6119	–3.0420	–3.1602
	15		–7.9722	–4.0299	–3.2446	–3.2258
	5	0	–4.9257	–3.1870	–3.0716	–3.0691
		0.1	–4.9722	–3.1940	–2.9850	–3.1260
		0.3	–5.0648	–3.2060	–2.8056	–3.2359
		0.5	–5.1568	–3.2156	–2.6184	–3.3405
		0.7	–5.2483	–3.2234	–2.4222	–3.4392

St (see Fig. 14). This is mainly due to the development of frictional drag for small time and as time passes and flow develops the inertial forces become pathetic therefore the frictional torque decreases.

The influence of amplitude ε on the velocity and the shear stress is demonstrated through Figs. 15 ~ 19. Figure 15 shows that for a fix value of t and increasing values of amplitude ε, the radial velocity decreases but far away from the disk the radial velocity increases. It is noted from Fig. 16 that the rotating velocity of fluid increases as ε increases but no exaggerated effect on the boundary-layer thickness has been observed. Figure 17 depicts the effect of amplitude ε on the radial velocity against the dimensionless time t. It can be perceived from the figure that as the values of ε fall off the amplitude of oscillations in the velocity profile is also diminished and for $\varepsilon = 0$ the results for linearly stretching and rotating disk are recovered. Figures 18 and 19 point out that as ε increases the amplitude of oscillation in wall shear force and the frictional torque also amplifies. Tables 1 and 2 illustrate the numerical values of the radial shear stress and frictional torque, respectively, for various values of ε. It is observed that both shear forces increases or decreases depending upon the time. However, it is observed that the amplitudes of oscillations in shear forces increase with ε. Figure 20 illustrates that the radial velocity near to the surface of disk is more oscillatory as compared to the velocity far away from the disk surface and tends to zero as one move away from the surface.

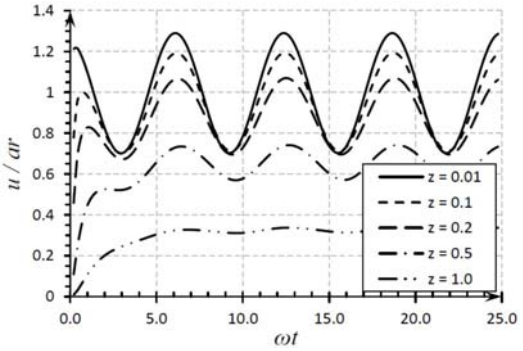


Fig. 20 Behavior of the radial velocity u in boundary layer region when $\Omega = 2$, $St = 5$ and $\varepsilon = 0.3$

5. CONCLUDING REMARKS

In this study, the unsteady boundary layer flow of a viscous fluid near an oscillatory stretching and rotating disk has been investigated numerically. Effects of swirl parameter on velocity, shear stress and frictional torque have been discussed in detail. It is concluded that these quantities are strongly dependent upon the swirl parameter Ω, the Strouhal number *St* and the amplitude of oscillations ε. It is observed that the involvement of swirl parameter strongly enhances the velocity in all three directions. The radial velocity of fluid increases as the swirling of disk increases. Moreover, the swirl parameter helps in enhancing the fluid velocity in axial and tangential directions. The amplitude of oscillation in radial velocity is more significant as compared to the tangential and axial velocities. It is concluded that the radial shear stress increases as the rotation rate increases. However, the frictional torque decreases as the rotation increases. It is also observed that as angular velocity of disk increases the influence of oscillations penetrates in the tangential velocity. The frictional torque decreases as the angular velocity of disk increases. The unsteady characteristic of the problem reveals that for very initial time radial shear force and the frictional torque are very small and increase with the passage of time. The contribution of the Strouhal number is to decrease the velocity profile and dominates the influence of unsteadiness on the flow and enhances the shear forces on the disk surface.

https://doi.org/10.1017/jmech.2014.37 Published online by Cambridge University Press

ACKNOWLEDGEMENTS

The authors are grateful to the anonymous reviewer for his expertise comments and suggestions in improving the quality of manuscript.

REFERENCES

1. Sakiadis, B. C., "Boundary-Layer Behavior on Continuous Solid Surfaces: I. Boundary-Layer Equations for Two-Dimensional and Axisymmetric Flow," *AIChE Journal*, **7**, pp. 26–28 (1961).
2. Crane, L. J., "Flow Past a Stretching Plate," *Zeitschrift Fur Angewandte Mathematik Und Physik*, **21**, pp. 645–647 (1970).
3. Wang, C. Y., "The Three-Dimensional Flow due to a Stretching Flat Surface," *Physics of Fluids*, **27**, pp. 1915–1916 (1984).
4. Banks, W. H. H., "Similarity Solutions of the Boundary-layer Equations for a Stretching," *Journal De Mecanique Theorique Et Appliquee*, **2**, pp. 375–392 (1983).
5. Kumari, M., Takhar, H. S. and Nath, G., "MHD Flow and Heat Transfer over a Stretching Surface with Prescribed Wall Temperature or Heat Flux," *Wärme - und Stoffübertragung*, **25**, pp. 331–336 (1990).
6. Grubka, L. J. and Bobba, K. M., "Heat Transfer Characteristics of a Continuous Stretching Surface with Variable Temperature," *Journal of Heat Transfer*, **107**, pp. 248–250 (1985).
7. Tamayol, A., Hooman, K. and Bahrami, M., "Thermal Analysis of Flow in a Porous Medium over a Permeable Stretching Wall," *Transport in Porous Media*, **85**, pp. 661–676 (2010).
8. Mehmood, A. and Ali, A., "Analytic Solution of Three-Dimensional Viscous Flow and Heat Transfer over a Stretching Flat Surface by Homotopy Analysis Method," *Journal of Heat Transfer*, **130**, 121701 (7 pages) (2008).
9. Munawar, S., Mehmood, A. and Ali, A., "Time-Dependent Flow and Heat Transfer over a Stretching Cylinder," *Chinese Journal of Physics*, 50, pp. 828–848 (2012).
10. Mehmood, A., Munawar, S. and Ali, A., Comments to: "Homotopy Analysis Method for Solving the MHD Flow over a Nonlinear Stretching Sheet, Commun. Nonlinear Sci. Numer. Simul.," *Communications in Nonlinear Science and Numerical Simulation*, **15**, pp. 4233–4240 (2010).
11. Wang, C. Y., "Nonlinear Streaming due to the Oscillatory Stretching of a Sheet in a Viscous Fluid," *Acta Mechanica*, **72**, pp. 261–268 (1988).
12. Rajagopal, K., Veena P. H. and Pravin, V. K., "Oscillatory Motion of an Electrically Conducting Viscoelastic Fluid over a Stretching Sheet in a Saturated Porous Medium With Suction/Blowing," *Mathematical Problems in Engineering*, Article ID 60560, pp. 1–14 (2006).
13. Abbas, Z., Wang, Y., Hayat, T. and Oberlack, M., "Slip Effects and Heat Transfer Analysis in a Viscous Fluid over an Oscillatory Stretching Surface," *International Journal for Numerical Methods in Fluids*, **59**, pp. 443–458 (2009).
14. Munawar, S., Mehmood, A. and Ali, A., "Unsteady Flow of Viscous Fluid over the Vacillate Stretching Cylinder," *International Journal for Numerical Methods in Fluids*, **70**, pp. 671–681 (2012).
15. Kármán, T. V., "Über Laminare und Turbulente Reibung," *ZAMM-Zeitschrift Fur Angewandte Mathematik Und Mechanik*, **1**, pp. 233–252 (1921).
16. Cochran, W. G., "The Flow due to a Rotating Disc," *Mathematical Proceedings of the Cambridge Philosophical Society*, **30**, pp. 365–375 (1934).
17. Stuart, J. T., "On the Effects of Uniform Suction on the Steady Flow Due to a Rotating Disk," *Quarterly Journal of Mechanics and Applied Mathematics*, **7**, pp. 446–457 (1954).
18. Sparrow, E. M. and Gregg, J. L., "Mass Transfer, Flow, and Heat Transfer about a Rotating Disk," *Journal of Heat Transfer*, **82**, pp. 294–302 (1960).
19. Kuiken, H. K., "The Effect of Normal Blowing on the Flow Near a Rotating Disk of Infinite Extent," *Journal of Fluid Mechanics*, **47**, pp. 789–798 (1971).
20. Ackroyd, J. A. D., "On the Steady Flow Produced by a Rotating Disc with Either Surface Suction or Injection," *Journal of Engineering Mathematics*, **12**, pp. 207–220 (1978).
21. Kakutani, T., "Hydromagnetic Flow Due to a Rotating Disk," *Journal of the Physical Society of Japan*, **17**, pp. 1496–1506 (1962).
22. Sparrow, E. M. and Chess, R. D., "Magnetohydrodynamic Flow and Heat Transfer about a Rotating Disk," *Journal of Applied Mechanics*, ASME, **29**, pp. 181–187 (1962).
23. Thacker, W. I., Kumar, S. K. and Watson, L. T., "Magnetohydrodynamic Flow and Heat Transfer about a Rotating Disk with Suction and Injection at the Disk Surface," *Computers and Fluids*, **16**, pp. 183–193 (1988).
24. Frusteri, F. and Osalusi, E., "On MHD and Slip Flow over a Rotating Porous Disk with Variable Properties," *International Communications in Heat and Mass Transfer*, **34**, pp. 492–501 (2007).
25. Ariel, P. D., "Axisymmetric Flow of a Second Grade Fluid Past a Stretching Sheet," *International Journal of Engineering Science*, **39**, pp. 529–553 (2001).
26. Sajid, M., Ahmed, I., Hayat, T. and Ayub, M., "Series Solution for Unsteady Axisymmetric Flow and Heat Transfer over a Radially Stretching Sheet," *Communications in Nonlinear Science and Numerical Simulation*, **13**, pp. 2193–2202 (2008).
27. Fang, T. and Zhang, J., "Flow Between two Stretchable Disks - An Exact Solution of the Navier-Stokes Equations," *International Communications in Heat and Mass Transfer*, **35**, pp. 892–895 (2008).
28. Munawar, S., Mehmood, A. and Ali, A., "Effects of

https://doi.org/10.1017/jmech.2014.37 Published online by Cambridge University Press

Slip on Flow between Two Stretchable Disks using Optimal Homotopy Analysis Method," *Canadian Journal of Applied Sciences*, **1**, pp. 50–68 (2011).
29. Fang, T., "Flow over a Stretchable Disk," *Physics of Fluids*, **19**, 128105 (2007).
30. Munawar, S., Mehmood, A. and Ali, A., "Time-Dependent Stagnation-Point Flow over Rotating Disk Impinging Oncoming Flow," *Applied Mathematics and Mechnics*, English Edition, **34**, pp. 85–96 (2013).

(Manuscript received February 26, 2013,
accepted for publication February 4, 2014.)

https://doi.org/10.1017/jmech.2014.37 Published online by Cambridge University Press